THE JOURNAL OF BIOLOGICAL CHEMISTRY
Vol. 277, No. 3, Issue of January 18, pp. 1855–1863, 2002

Printed in U.S.A.

Localization of Phosphatidylserine Binding Sites to Structural Domains of Factor X_a*

Received for publication, June 20, 2001, and in revised form, October 12, 2001
Published, JBC Papers in Press, November 13, 2001, DOI 10.1074/jbc.M105697200

Arvind Srivastava‡, Jianfang Wang‡, Rinku Majumder‡, Alireza R. Rezaie§, Johan Stenflo¶, Charles T. Esmon‖, and Barry R. Lentz‡

From the ‡Department of Biochemistry & Biophysics, University of North Carolina, Chapel Hill, North Carolina 27599-7260, the ¶Department of Clinical Chemistry, University of Lund, Malmö General Hospital, Malmö S214 01, Sweden, the §Department of Biochemistry and Molecular Biology, St. Louis University School of Medicine, St. Louis, Missouri 63104, and the ‖Department of Biochemistry and Biophysics and Pathology, Oklahoma Medical Research Foundation, University of Oklahoma Health Sciences Center and Howard Hughes Medical Institute, Oklahoma City, Oklahoma 73104

Binding of short chain phosphatidylserine (C6PS) enhances the proteolytic activity of factor X_a by 60-fold (Koppaka, V., Wang, J., Banerjee, M., and Lentz, B. R. (1996) *Biochemistry* 35, 7482–7491). In the present study, we locate three C6PS binding sites to different domains of factor X_a using a combination of activity, circular dichroism, fluorescence, and equilibrium dialysis measurements on proteolytic and biosynthetic fragments of factor X_a. Our results demonstrate that the structural responses of human and bovine factor X_a to C6PS binding are somewhat different. Despite this difference, data obtained with fragments from both human and bovine factor X_a are consistent with a common hypothesis for the location of C6PS binding sites to different structural domains. First, the γ-carboxyglutamic acid (Gla) domain binds C6PS only in the absence of Ca^{2+} ($k_d \sim 1$ mM), although this PS site does not influence the functional response of factor X_a. Second, a Ca^{2+}-dependent binding site is in the epidermal growth factor domains (EGF_{NC}) that are linked by Ca^{2+} and C6PS binding to the Gla domain. This site appears to be the lipid regulatory site of factor X_a. Third, a Ca^{2+}-requiring site seems to be in the EGF_C-catalytic domain. This site appears not to be a lipid regulatory site but rather to share residues with the substrate recognition site. Finally, the full functional response to C6PS requires linkage of the Gla, EGF_{NC}, and catalytic domains in the presence of Ca^{2+}, meaning that PS regulation of factor X_a involves linkage between widely separated parts of the protein.

The substantial effects of soluble phosphatidylserine (C6PS[1]) on the kinetics of prothrombin activation by factor X_a (1) and on the structure of factor X_a, as documented here, indicate that phosphatidylserine (PS) may act as an allosteric regulator of prothrombin activation. PS located on the cytoplasmic face of resting platelet plasma membranes is exposed on the surface of activated platelet vesicles (2, 3). The implication of this PS exposure and of the effect of PS on factor X_a and on its ability to catalyze activation of prothrombin is that PS may act as a second messenger in regulating thrombin formation. Because of the crucial role of thrombin in hemostasis, the exposure of PS may be a crucial regulatory step in blood coagulation. To better define this regulatory process, it is important to know the locations of the PS binding sites on factor X_a.

The organization of factor X into structural domains is illustrated below in Fig. 1. Factor X consists of two peptides. The *light chain* consists of an N terminus γ-carboxyglutamic acid-rich region (Gla module) and two Cys-rich cassette modules. The *heavy chain* consists of the serine protease catalytic domain. The two cassette modules of the light chain show strong sequence and structural homology to epidermal growth factor (EGF) (4) and are thus referred to as EGF_N and EGF_C, where N and C indicate the domain nearer to the N and C termini, respectively. Crystal structures of Gla domain-less factor X_a ($GDFX_a$) have been published (5–7). In the most recent of these (7), the EGF cassette modules extend from the catalytic domain to make an extended molecule. In the structure of the analogous serine protease, factor IX_a, the EGF_N module is bent at the inner-EGF_C hinge region to right angles with the EGF_C, which is tucked along the catalytic module (8). It may be that the EGF modules form a hinge region that modulates the global structure of factor X_a. The factor IX_a structure also differs from that of $GDFX_a$ in containing the Gla domain. Although the Gla domain is critical for membrane binding and may modulate the structure of the EGF modules, little is known about the structure of Gla in whole factor X_a. We have only a model structure of factor X_a Gla domain based on the prothrombin Gla domain (9).

Binding of Ca^{2+} to factor X is reportedly required for activation by factor VII_a/tissue factor or by factor IX_a/$VIII_a$ (10, 11)

* This work was supported by Grants HL45916 (to B. R. L.), HL62565 (to A. R. R.), and P01 HL54804 (to C. E.) from the United States Public Health Services and by the Swedish Medical Research Council (to J. S.). The costs of publication of this article were defrayed in part by the payment of page charges. This article must therefore be hereby marked "*advertisement*" in accordance with 18 U.S.C. Section 1734 solely to indicate this fact.

** To whom correspondence should be addressed: Dept. of Biochemistry & Biophysics, University of North Carolina, MEJB 7260, Chapel Hill, NC 27599-7260. Tel.: 919-966-5384; Fax: 919-966-2852; E-mail: uncbrl@med.unc.edu.

[1] The abbreviations used are: C6PS, 1,2-dicaproyl-*sn*-glycero-3-phospho-L-serine; C6PC, 1,2-dicaproyl-*sn*-glycero-3-phosphocholine; PS, phosphatidylserine; CD, circular dichroism; $\Theta_{222}/\Theta_{208}$, ellipticity ratio at wavelength 222 to 208 nm; RVV-X, Russel's viper venom factor X-activating protein; PEG, polyethylene glycol; S-2765, *N*-α-benzyloxycarbonyl-D-arginyl-L-glycyl-L-arginine-*p*-nitroanilide dihydrochloride; SpPCa, Spectrozyme PCa; Gla, N-terminus γ-carboxyglutamic acid-rich region; EGF_N, epidermal growth factor nearest to the N terminus; EGF_C, epidermal growth factor nearest the C terminus; Gla-EGF_N, Gla domain linked to the epidermal growth factor EGF_N; Gla-EGF_{NC}, Gla domain linked to both epidermal growth factors EGF_N and EGF_C; E_2FX_a, factor X_a construct lacking both the Gla and the EGF_N domains; DEGR, [5-(dimethylamino)-1-napthalenesulfonyl]glutamylycylarginyl chloromethyl ketone; $GDFX_a$, factor X_a construct missing the Gla domain; Y99T, $GDFX_a$ mutant in which Tyr-99 is replaced with Thr; CMC, critical micelle concentration.

and for the activity of factor X_a (12). Ca^{2+} binding is also required for PS regulation of factor X_a proteolytic activity (1). Ca^{2+} binds mainly to the Gla module (13), but there also appears to be a high affinity Ca^{2+} binding site ($k_d \sim 160$ μM) in the catalytic domain (9, 14–16) and a lower affinity Ca^{2+} binding site ($k_d \sim 0.7$–1.2 m M) on the isolated first EGF-like module (4, 12, 16, 17). A Ca^{2+}-dependent interaction between the EGF-like and Gla modules appears to enhance the affinity of the site on the EGF-like module to the point that it is tighter (17, 18) ($k_d \sim 120$ μM) than the catalytic domain site. Consistent with this, nuclear magnetic resonance shows that Ca^{2+} binding tightens the fold of the isolated EGF_N domain and bends Gla and EGF_N domains toward each other around a hinge located in the Gla domain, referred to as a *helical* or *hydrophobic stack* (19).

Despite considerable information about Ca^{2+} binding to factor X_a, we have virtually no information about the location of PS binding sites on this key enzyme. The aims of this work have been to locate the lipid regulatory site(s) in factor X_a and to identify the structural domains of factor X_a necessary to see the C6PS regulatory effect on factor X_a activity.

EXPERIMENTAL PROCEDURES

Materials

1,2-Dicaproyl-*sn*-glycero-3-phospho-L-serine (C6PS) and 1,2-dicaproyl-*sn*-glycero-3-phosphocholine (C6PC) were purchased from Avanti Polar Lipids Inc. (Alabaster, AL). Russel's viper venom factor X-activating protein (RVV-X) was purchased from Hematological Technologies Inc. (Essex Junction, VT), and factor X_a-specific substrate *N*-α-benzyloxycarbonyl-D-arginyl-L-glycyl-L-arginine-*p*-nitroanilide dihydrochloride (S-2765) was purchased from Helena Laboratories (Beaumont, TX). Chymotrypsin was purchased from Worthington (Lakewood, NJ). Chromogenetic substrate Spectrozyme PCa (SpPCa) was purchased from American Diagnostica (Greenwich, CT). [5-(Dimethylamino)-1-napthalenesulfonyl] glutamylycylarginyl chloromethyl ketone (DEGR-CK) was purchased from Calbiochem (La Jolla, CA). Diisopropyl fluorophosphate was purchased from Sigma Chemical Co. (St. Louis, MO). All other chemicals were ACS reagent grade or the best available grade.

Methods

Preparation of Factor X_a—Bovine factor X was isolated from a barium citrate precipitate obtained from freshly collected bovine plasma (20, 21). Human factor X for stoichiometry and CD measurements was purified from recovered human plasma obtained from the American Red Cross, according to the method of Dahlback *et al.* (22). Factor X obtained as above was analyzed by SDS-PAGE, concentrated (Centricon-10 concentrator supplier), and then stored at −70 °C at a concentration of about 1 mg/ml in 5 mM Tris, 20 mM sodium citrate, 0.6 M NaCl, pH 7.4. A final purification of factor X was performed 1 day before an experiment by high-performance liquid chromatography on a PerkinElmer Life Sciences Isopure LC system using a Mono Q HR 5/5 ion exchange column (Amersham Biosciences, Inc., Norwalk, CN). The purified factor X was dialyzed into buffer (50 mM Tris, 175 mM NaCl, pH 7.4) for activation. Factor X (10 μM) with 5 mM Ca^{2+} was activated at 25 °C with RVV-X that had been covalently linked to agarose beads (10, 23). Factor X_a was purified by high-performance liquid chromatography on a Mono Q column, and the isolated protein was analyzed by SDS-PAGE electrophoresis. Factor X_a concentration was measured by determining the rate of S-2765 hydrolysis in a plate reader-based assay (1), using active site-titrated factor X_a to construct the standard curve (24).

Purification of Domain Fragments of Bovine Factor X_a—Isolation and purification of fragments of bovine factor X_a and several of its structural domains (Gla, EGF_N, Gla-EGF_N, and Gla-EGF_{NC}) by controlled trypsin digestion were described previously (18, 25, 26).

Preparation of GDFX$_a$, E$_2$FX$_a$, and Y99T—The RSV-PL4 expression vector was used to express factor X, GDFX, and a construct missing both the Gla and first EGF domain (E_2FX) in human 293 cells (16). GDFX was also prepared for stoichiometry measurements as described by Morita and Jackson (27) from isolated factor X. Purified factor X was reacted with α-chymotrypsin (1:400 factor X:α-chymotrypsin) at 22 °C for 45 min, a time sufficient to convert 95% of factor X to GDFX, as judged by SDS-PAGE on a 6% gel. The reaction was stopped by addition of 1 mM diisopropyl fluorophosphate, and Gla-domainless factor X was chromatographed on a Mono Q column. GDFX Y99T mutant was also prepared as described (28–30). GDFX and its mutant and E_2FX were activated with RVV-X as described earlier (29).

Measurement of Amidolytic Activity of Factor X_a and Its Constructs—The amidolytic activities of expression products of a human factor X_a cDNA and of expression products of two of its deletion mutants ($GDFX_a$, E_2FX_a) were measured in the presence of 3 mM Ca^{2+} using the synthetic substrate S-2765 and the microplate reader-based assay described above. Samples, containing 20 nM protein, various concentrations of C6PS and 3 mM Ca^{2+} in a buffer (50 mM Tris, 175 mM NaCl, pH 7.6) containing 0.6% PEG, were incubated at 37 °C for 15 min before measuring activities. The amidolytic activities were estimated from measured initial rates of S-2765 hydrolysis, using a standard curve obtained with active site-titrated factor X_a (1). Amidolytic activities of $GDFX_a$ and Y99T were measured using the chromogenetic substrate Spectrozyme PCa (SpPCa) also as described earlier (29). Samples containing 20 nM protein, various concentrations of C6PS (0, 400, 900 μM), and 0.6% PEG (to prevent adsorption of protein to the plate) were incubated in buffer (50 mM Tris, 175 mM NaCl, pH 7.6) in polypropylene Eppendorf tubes at 37 °C for 5 min before being added to a flat-bottomed polypropylene 96-well plate (Greiner America, Inc.) preincubated at 37 °C. The initial rates of SpPCa amidolysis were determined on a Versamax Tunable Microplate Reader (Molecular Devices, Sunnyvale, CA) at five substrate concentrations (50, 100, 200, 400, and 600 μM) and analyzed in terms of the Michaelis-Menten model using non-linear regression methods available in Sigma Plot 6.0.

Circular Dichroism Measurements—Circular dichroism (CD) spectra were generally recorded from 250 to 200 nm on an Aviv Model 620S spectrometer (Aviv Associates, Inc., Lake Wood, NJ) in a 1-cm path-length cell at 24 °C with a bandwidth of 1.0 nm. Data points were collected at every 0.5 nm with an average time of 5 s on each point. Some data were obtained down to 195 nm on an Applied Photophysics P_i* spectrometer in a 1-mm path-length cell with a bandwidth of 1 nm and data collection at every 0.5 nm. Baseline CD spectra of buffer containing various concentrations of soluble C6PS were collected in the absence and in the presence of 3 mM Ca^{2+} and were subtracted from sample spectra. The baseline-corrected digital data were processed, smoothed, and converted to molar ellipticity, $\Delta\Theta$. We have previously determined the critical micelle concentration (CMC) of C6PS at different Ca^{2+} and protein concentrations (1), but controls to detect micelle formation were in all cases still performed by watching for sudden drops in ellipticity in the range of 240–250 nm. For human and bovine factor X_a,[2] the CMC seen in this way was similar to the CMC reported earlier by quasi-elastic light scattering methods (1). The ellipticity ratio $\Theta_{222}/\Theta_{208}$ (32) is used here as a convenient parameter to follow changes in the secondary structure of factor X_a and its fragments upon addition of C6PS. In addition, we have estimated α-helix content using published software packages CDSSTR and CONTIN (33) to give context to the $\Theta_{222}/\Theta_{208}$ ratio. The ability of CD spectra taken to 200 nm to define α-helix content but not β-sheet or turn content is well documented (34). We could not collect spectra to 185 nm to perform a complete secondary structure analysis in a buffer containing NaCl, because Na^+ increases the buffer absorbance in the deep UV (34). Na^+ was necessary in our studies, because Ca^{2+} binding is required for regulation of factor X_a by C6PS (1), and Ca^{2+} binding is linked to Na^+ binding (35, 36).

Fluorescence Titration of DEGR-E$_2$FX$_a$ by Soluble C6PS—Fluorescence intensity measurements were carried out on an SLM 48000 spectrofluorometer (SLM Aminco, Urbana, IL). Slits were closed between measurements to avoid photodegradation of the sample. All buffer solutions were filtered using 0.2-μm filters (Nalge Co., Rochester, NY). DEGR-E_2FX_a was prepared by sequential addition of 5 μl of DEGR-CK (1 mg/ml in 0.02 M Tris, 0.1 M NaCl, pH 7.5) to 1 ml of about 1 μM purified factor E_2FX_a. The extent of labeling at the active site was followed by the loss of enzymatic activity, as monitored by the S-2765 assay. Labeling was stopped when no activity remained. DEGR-E_2FXa was then dialyzed against 50 mM Tris, 0.1 M NaCl, pH 7.5, to remove free reagent (37). DEGR-E_2FX_a (100 nM) in 1.0 ml of buffer (50 mM Tris, pH 7.5) was incubated in a stirred micro-cuvette (Hellma Cells, Jamaica, NY) with 0.15 mM NaCl or 3 mM Ca^{2+} or both at 25 °C for 20 min. Following additions of C6PS (1–2 μl each addition for a maximum of 4% dilution) and an equilibration of at least 4 min, fluorescence intensity was recorded using an excitation wavelength of 340 nm (bandpass 8 nm) and an emission wavelength of 550 nm (bandpass 4 nm). For each addition, several intensity measurements were performed and averaged and corrected for dilution. Control experiments were per-

[2] J. Wang, R. Majumder, and B. R. Lentz, submitted for publication.

formed in which buffer was titrated with soluble lipid in the absence of protein. The lipid solution showed very minor background fluorescence or light scattering signal (which was subtracted from sample signal) until the critical micelle concentration was reached. The critical micelle concentration for C6PS in the presence and absence of 1 μM factor X_a were determined previously to be 0.95 and 2.5 mM, respectively (1). The critical micelle concentrations for C6PC under similar conditions were even higher (1). Data were not analyzed above the critical micelle concentration.

Intrinsic Fluorescence of Gla-EGF$_{NC}$—Gla-EGF$_{NC}$ (100 nM) in 50 mM Tris, 150 mM NaCl, pH 7.4, in the presence and in absence of 3 mM Ca^{2+} was titrated with soluble C6PS, and the intrinsic fluorescence was monitored at 345 nm (bandpass 4 nm) followed by excitation at 285 nm (bandpass 8 nm). Control experiments were as mentioned for DEGR-E_2FX_a fluorescence.

Phospholipid Sample Preparation—C6PS and C6PC solutions were prepared from measured quantities of 10 mg/ml stock solutions in chloroform. The chloroform was evaporated under a stream of nitrogen. The lipid was re-dissolved in cyclohexane, and this solution was frozen on the wall of a capped test tube and then lyophilized overnight. The resulting dry powder was dispersed in the appropriate volume of buffer and vortexed thoroughly to reach a concentration of ~100 mM. The final concentration of this phospholipid stock solution was determined by an inorganic phosphate assay (38).

Determination of the Stoichiometry of C6PS Binding to Various Fragments of Factor X_a—The stoichiometries of soluble C6PS binding to factor X_a, GDFX$_a$, Gla-EGF$_{NC}$, and Gla in the absence and in the presence of 3 mM Ca^{2+} were determined by equilibrium dialysis measurements. This procedure not only establishes stoichiometry but also confirms indirect binding results by a direct measurement. Experiments were performed using 2.0-ml Teflon dialysis cells (Spectrum Medical, Los Angeles, CA) with the two cells separated by a 2000 molecular weight cut-off membrane. Both chambers contained equal amounts of C6PS, enough to saturate >85% of the protein present in one-half of the dialysis cell at varying concentrations (30–100 μM). The lipid concentrations used depended on the crude binding constants estimated in CD titrations. Depending on the particular combination of lipid and protein concentration in a given experiment and on the stoichiometry of binding for a particular peptide, between 79 and 94% of lipid remained unbound at equilibrium. The two chambers were allowed to equilibrate at room temperature for 24 h while being rotated horizontally at 20 rpm. The protein concentration gradient between the two halves of the cell causes a difference in the total phosphate concentration between the two halves of the cell. The concentration of protein-bound C6PS was measured as the difference in total phosphate concentration (ΔP) (38) between the two chambers of the dialysis cell. Assuming a simple model of binding of lipid to n equivalent and independent sites, it is easy to show that ΔP should vary with protein concentration as follows,

$$\Delta P = \frac{[L]n[P]}{\frac{k_d}{n} + [L]} \quad \text{(Eq. 1)}$$

where $[L]$ is free lipid concentration and k_d/n is the observed stoichiometric dissociation constant for lipid binding, assuming a single site model. For $[L] \gg k_d/n$, this is roughly a straight line with a slope proportional to n. In our experiments, we maintained $[L] > k_d/n$, but the total lipid concentration had to remain less than the CMC of the lipid. Thus, to obtain n, we had to fit a plot of ΔP *versus* protein concentration to the non-linear equation given in Equation 1, using standard non-linear regression procedures and the program SigmaPlot (version 6 for Windows 2000; Jandel Scientific).

Data Analysis

In our experiments, soluble lipid was added to the protein solution, and the observed response was taken as representing the fraction of protein bound (f) to lipid at concentration $[L]$ given by,

$$f = \frac{[L]}{K_d + [L]} \quad \text{(Eq. 2)}$$

where K_d is the apparent stoichiometric binding constant for soluble lipid binding to the protein. Any observable value that changes from an initial value of R_0 to a final value at saturation, R_{sat}, as a result of binding can be written as follows,

$$\frac{R}{R_0} = 1 + \frac{R_{sat} - R_0}{R_0} \times f \quad \text{(Eq. 3)}$$

RESULTS

Effect of Soluble C6PS on the Amidolytic Activities of Human Factor X_a and Its Deletion Constructs—We have shown previously that C6PS enhances proteolytic activity of human factor X_a by roughly 60-fold but inhibits the amidolytic activity toward S-2765 by 60% (1). The variation of amidolytic activity of expressed human factor X_a, GDFX$_a$, and E_2FX_a (Fig. 1) in the presence of 3 mM Ca^{2+} with soluble C6PS concentration is shown in Fig. 2. The highest C6PS concentration used (0.8 mM) was still below the CMC for C6PS in the presence of 3 mM Ca^{2+} (~2.5 mM) (1). The amidolytic activities of factor X_a and GDFX$_a$ were decreased by 79 and 9%, respectively, at saturation with C6PS (Table I), but C6PS had negligible effect on the amidolytic activity of E_2FX_a. The functional responses of factor X_a and its constructs to C6PS binding were reasonably well described by a single binding site model (see "Methods"), and the binding parameters are given in Table I. The apparent K_d for C6PS binding to the expressed human factor X_a in this experiment (39 ± 6 μM) was comparable to but somewhat smaller than we have reported previously for factor X_a isolated from outdated human plasma (65 ± 5 μM) (1), and the percent inhibition was also greater (80 *versus* 60%). This probably reflects the slight difference between X_a from human plasma and factor X_a from a single cDNA clone, as used here.

Effect of Soluble C6PS on the CD Spectra of Expressed Human Factor X_a and Its Constructs—The effects of soluble C6PS on the CD spectra of expressed human factor X_a and its constructs, GDFX$_a$ and E_2FX_a, were studied in the absence and presence of 3 mM Ca^{2+}. CD spectra of human factor X_a are shown at various concentrations of C6PS in the presence (Fig. 3*A*) and in the absence of 3 mM Ca^{2+} (Fig. 3*B*). Although it is reported to bind Ca^{2+} (17), human factor X_a did not undergo a detectable change in secondary structure upon addition of 3 mM Ca^{2+}, as seen from the *solid* and *dotted curves* in Fig. 3*A* and from the $\Theta_{222}/\Theta_{208}$ ratio and α-helical content (Table I). Secondary structure analysis yielded an estimate of 11% helical content in the presence or absence of Ca^{2+}, in good agreement with the reported helicity for the analogous factor IX_a crystal structure (10.6%) (8). However, there was a substantial change in CD upon addition of C6PS to human factor X_a in the presence of 3 mM Ca^{2+} (Fig. 3*A*). By contrast, there was only a small change in CD upon addition of C6PS in the absence of Ca^{2+}. The variation of ellipticity ratio ($\Theta_{222}/\Theta_{208}$) for human factor X_a with C6PS concentration is shown as an *inset* in Fig. 3 (*A* and *B*) in the presence and absence of Ca^{2+}, respectively.

The variations of ellipticity ratio of GDFX$_a$ and E_2FX_a with C6PS concentration are shown in Fig. 4 (*B* and *C*, respectively). The smooth lines through the data result from fitting the data to a single-binding-site model as described under "Methods." The stoichiometric binding constants (K_d) and percent changes in $\Theta_{222}/\Theta_{208}$ at saturation ($\Delta R_{sat}/R_0 \times 100\%$), resulting in the least square fits, are reported in Table II. We stress that K_d values obtained in this way cannot be interpreted as site binding constants (k_d), because the number of data points taken and their intrinsic accuracy were not sufficient to define a binding mechanism in terms of the number, affinities, and responses of different sites present on each peptide fragment. However, the data in Fig. 4 do establish, in most cases, which fragments do bind C6PS, the magnitude of the total response (shifts in secondary structure), and the fraction of sites occupied at any lipid concentration (from K_d values). The ellipticity ratio of factor X_a decreased by 6% upon saturation with C6PS in the absence of Ca^{2+} and by 16% when saturated with C6PS in the presence of 3 mM Ca^{2+}. Similarly, the α-helical content decreased by 1 and

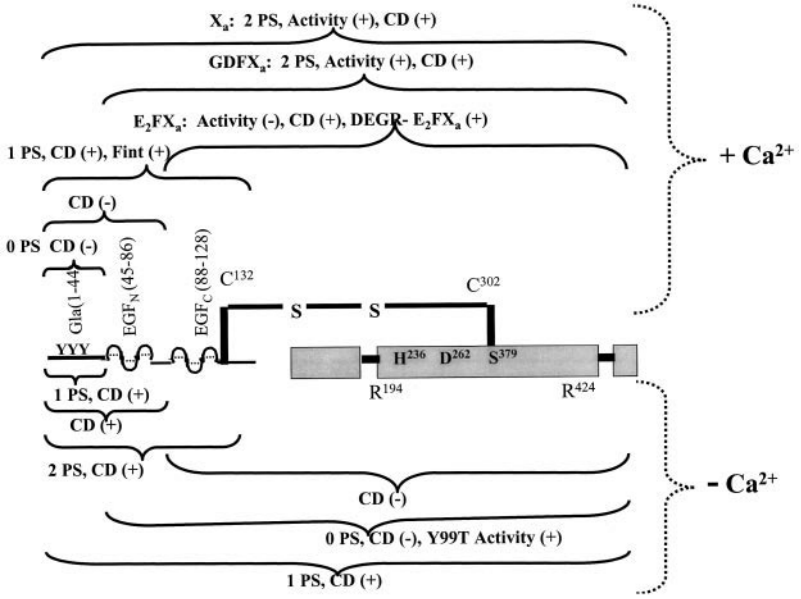

FIG. 1. **Domain structure of factor X_a and summary of results.** Schematic diagram of the domain structure of human factor X_a. The N terminus contains a region rich in γ-carboxyglutamic acid responsible for membrane binding (Gla domain). The epidermal growth factor domains (EGF_N and EGF_C) and the catalytic domain are also shown. The construct missing the Gla domain is referred to as *$GDFX_a$*, and the domain missing both the Gla and EGF_N domains is called *E_2FX_a*. Results in the absence of Ca^{2+} are summarized *below the factor X_a diagram*: bovine Gla, Gla-EGF_N, and Gla-EGF_{NC} CD spectra all responded to C6PS. Stoichiometry measurements showed that Gla domain binds to one molecule of C6PS, whereas the Gla-EGF_{NC} domain binds to two molecules. Neither stoichiometry nor CD measurements showed an interaction of C6PS with human E_2FX_a or $GDFX_a$. Factor X_a binds one molecule of C6PS, an interaction confirmed by CD. Results in the presence of Ca^{2+} are summarized *above the factor X_a diagram*: bovine Gla and Gla-EGF_N did not bind to C6PS, but Gla-EGF_{NC} binds one molecule of C6PS and also showed a change in CD spectrum and intrinsic fluorescence with C6PS. Human E_2FX_a, $GDFX_a$, and factor X_a all showed altered CD spectra with C6PS. $GDFX_a$ and factor X_a each bind two molecules of C6PS, and their amidolytic activities were sensitive to the presence of C6PS. Although E_2FX_a binding to C6PS was detected with CD and fluorescence, its amidolytic activity was unchanged with the addition of C6PS.

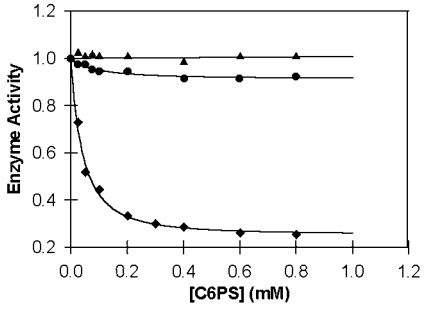

FIG. 2. **The effect of soluble C6PS on amidolytic activities of human factor X_a and its constructs, $GDFX_a$ and E_2FX_a.** The initial rates of S-2765 amidolysis by factor X_a (*hexagons*), $GDFX_a$ (*circles*), and E_2FX_a (*triangles*) are plotted as a function of C6PS concentrations in the presence of 3 mM Ca^{2+}. Rates were measured at 37 °C in a buffer containing 50 mM Tris, 175 mM NaCl, 0.6% PEG, at pH 7.6. Absolute amidolytic activities of human factor X_a, $GDFX_a$, and E_2FX_a in the absence of C6PS were 1.40, 0.83, and 0.79 mM S-2765/s/μM enzyme, respectively. The absolute activities were calculated based on an extinction coefficient for S-2765 of 1.39 OD/μM at 405 nm.

TABLE I
Parameters describing binding of soluble C6PS to human factor X_a and its constructs in terms of changes in amidolytic activity

Protein/domain	K_d[a]	ΔR_{sat}[b]
	μM	
Human X_a	39 ± 6	−79
Human $GDFX_a$	86 ± 18	−9
Human E_2FX_a	NA[c]	0

[a] K_d, apparent stoichiometric dissociation constant.
[b] ΔR_{sat}, percent change in activity upon addition of saturating concentration of C6PS.
[c] NA, not applicable.

3%, respectively (Table II). There was an 18% decrease in $\Theta_{222}/\Theta_{208}$ ratio of $GDFX_a$ but only a slight (0.8%) decrease in helical content in response to soluble C6PS in the presence of 3 mM Ca^{2+}. This discrepancy between changes in $\Theta_{222}/\Theta_{208}$ and helical content suggests that $GDFX_a$ binding to C6PS involves more than a change in helical content. Neither the $\Theta_{222}/\Theta_{208}$ ratio nor the α-helix content changed upon addition of C6PS in the absence of Ca^{2+}(Fig. 4*B*, Table I). Human $GDFX_a$ seems to bind soluble C6PS in the presence of 3 mM Ca^{2+}, with its structural response being comparable to that of whole human factor X_a, but seems not to bind C6PS in the absence of Ca^{2+}, at least not with a measurable structural response. The $\Theta_{222}/\Theta_{208}$ ratio of E_2FX_a decreased by 10% upon addition of saturating concentrations of C6PS in the presence of 3 mM Ca^{2+} but remained unchanged in the absence of Ca^{2+}. The 10% decrease in ellipticity ratio was significantly smaller than that seen either for native human factor X_a (16%) or for $GDFX_a$ (16%).

Effect of Soluble C6PS on the CD Spectra of Bovine Factor X_a and Its Domains—The CD spectra of bovine factor X_a and its Gla, EGF_N, Gla-EGF_N, and Gla-EGF_{NC} domains were also collected and analyzed in terms of $\Theta_{222}/\Theta_{208}$ and α-helical content. The variations of ellipticity ratio ($\Theta_{222}/\Theta_{208}$) with C6PS concentration in the presence (*closed circles*) and absence (*open circles*) of 3 mM Ca^{2+} for factor X_a, Gla, Gla-EGF_N, and Gla-EGF_{NC} domains, are shown in Fig. 4 (*A*, *D*, *E*, and *F*, respectively). The smooth curves through these data result from fitting the data to a single-site binding model (see "Methods"), with binding constants (K_d) and fractional changes in $\Theta_{222}/\Theta_{208}$ at saturation (ΔR_{sat}) reported in Table II. The $\Theta_{222}/\Theta_{208}$ ratio of bovine factor X_a decreased by 16% upon addition of saturating concentration of C6PS in the absence of Ca^{2+} but increased by 26% in the presence of 3 mM Ca^{2+} (Table II). These same spectra were analyzed to reveal changes in α-helical content of −1 and +6%, respectively (Table II).

Comparison of changes in α-helical content with changes in $\Theta_{222}/\Theta_{208}$ ratios for human and bovine factor X_a and their

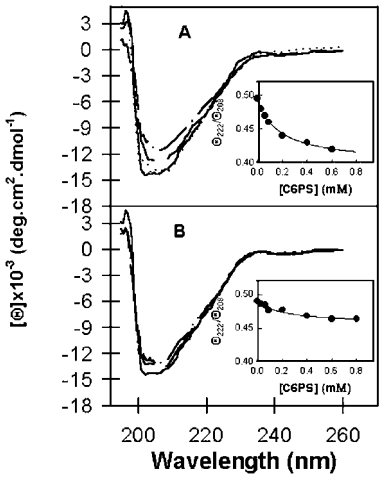

FIG. 3. *A*, the effect of C6PS on the CD spectrum of human factor X_a in the presence of 3 mM Ca^{2+}. Human factor X_a (0.6 μM) was examined at 24 °C in 1.0 mM Tris, 150 mM NaCl, pH 7.4, buffer (*solid line*), and in the presence of 3 mM Ca^{2+} (*dotted line*), 3 mM Ca^{2+} plus either 0.2 mM C6PS (*dashed line*) or 0.6 mM C6PS (*dot-dashed line*). The CMC of C6PS under the conditions of this experiment was estimated to be between 600 and 800 μM, based on changes in the ellipticity between 245 and 250 nm (see "Methods"). The variation of $\Theta_{222}/\Theta_{208}$ with C6PS in the presence of 3 mM Ca^{3+} is shown in the *inset*. *B*, the effect of C6PS on the CD spectrum of human factor X_a in the absence of Ca^{2+}. Human factor X_a (0.6 μM) was examined as above in the presence of 0 mM (*solid line*), 0.2 mM C6PS (*dashed line*), or 0.6 mM C6PS (*dot-dashed line*), but in the absence of Ca^{2+}. The variation of $\Theta_{222}/\Theta_{208}$ with C6PS in the absence of Ca^{3+} is shown in the *inset*. *Solid lines* shown in the *insets* result from fitting the data to a single-binding-site model ("Methods") with the best-fit parameters given in Table II.

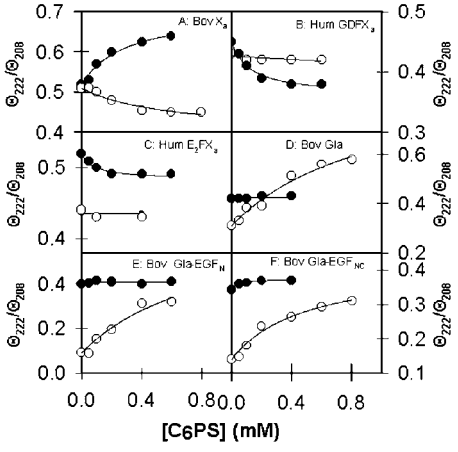

FIG. 4. **The variations of ellipticity ratio ($\Theta_{222}/\Theta_{208}$) with C6PS concentration.** *A*, bovine factor X_a; *B*, human $GDFX_a$; *C*, human E_2FX_a; *D*, bovine Gla; *E*, bovine Gla-EGF_N; *F*, bovine Gla-EGF_{NC}. In each panel, data are presented as collected in the presence of 3 mM Ca^{2+} (*filled circles*) and in the absence of Ca^{2+} (*open circles*). *Solid lines* show the results of fitting the data to a single-binding-site model ("Methods") with the best-fit parameters given in Table II.

fragments (Table II) makes it clear that there is a general correlation between these two parameters, but that the $\Theta_{222}/\Theta_{208}$ ratio reflects more than just helical content. It is also clear from comparison of the responses of bovine and human factor X_a to C6PS that the secondary structural changes associated with C6PS binding are different for these two proteins (Table II). However, CD spectra for bovine X_a taken under the same conditions used for the spectra in Fig. 3 were qualitatively similar to the human X_a spectra shown in Fig. 3. To make a more quantitative comparison of these two proteins, we collected spectra down to 185 nm in a buffer identical to that used for Fig. 3, except it lacked NaCl and was therefore much more

TABLE II
Parameters describing binding of soluble lipids to various domains of human and bovine factor X_a in the presence and absence of 3 mM Ca^{2+}

Protein/domain	K_d	Δ_{sat}[a]	(Helix change)$_{sat}$[b]
	μM		%
3 mM Ca^{2+}			
Human X_a	31 ± 10[c]	−16	11.1→8.2
Bovine X_a	304 ± 16[c]	+26	11.3→17.0
Human $GDFX_a$	130 ± 10[c]	−18	6.1→5.3
Human E_2FX_a	88 ± 8[c]	−10	6.1→5.6
Bovine Gla-EGF_{NC}	155 ± 12[c]	+10	10.1→11.2
Bovine Gla-EGF_N	NA[d]	0	9.2→9.1
Bovine EGF_N	NA[d]	0	6.0→5.9
Bovine Gla	NA[d]	0	15.6→15.9
No Ca^{2+}			
Human X_a	61 ± 8[c]	−6	11.0→10.1
Bovine X_a	584 ± 22[c]	−16	11.1→10.0
Human $GDFX_a$	NA[d]	0	6.0→5.9
Human E_2FX_a	NA[d]	0	6.1→6.1
Bovine Gla-EGF_{NC}	486 ± 18[c]	+121	9.7→12.5
Bovine Gla-EGF_N	852 ± 19[c]	+333	8.7→11.0
Bovine EGF_N	NA[d]	0	5.8→5.8
Bovine Gla	960 ± 28[c]	+97	13.8→15.9

[a] Calculated as the percent change in observable at saturating lipid, *i.e.* $\Delta_{sat} = (R_{sat} - R_0)/R_0 \times 100\%$. $R = \Theta_{222}/\Theta_{208}$.
[b] Changes in the percent helicity estimated by fitting the CD spectra by two different algorithms (33). The disparity between estimates by the two methods was always <10% of the estimates.
[c] Parameter uncertainty based on non-linear regression.
[d] NA, not applicable.

transparent in the deep UV spectrum (34). Dialysis of bovine factor X_a into this buffer and then return to a normal 150 mM NaCl buffer over a period of 48 h had no measurable effect on the ability to bind C6PS or on the amidolytic activity of factor X_a toward S-2765 substrate. Secondary structure analysis of the bovine and human protein spectra in a NaCl-free buffer revealed no difference between the two of greater than 0.9% of helical, beta, turn, or unstructured content. As expected, because Na^+ is needed for Ca^{2+} binding (35, 36) and Ca^{2+} is needed for C6PS binding (1), there was no significant change in secondary structure content upon addition of either Ca^{2+} or C6PS to either protein in the buffer lacking NaCl. Thus, spectra of this quality could not be used to quantitate the different effects of C6PS on bovine and human factor X_a secondary structure, but were useful to establish the expected structural similarity between these two analogous proteins.

The ellipticity ratio of the Gla domain increased by 43%, while α-helicity increased by 1.8% upon addition of 3 mM Ca^{2+} (Fig. 4*D* at 0 mM C6PS). In the absence of Ca^{2+}, the ellipticity ratio increased by 97% at saturation with C6PS while α-helicity increased by 2.1% (Table II). However, no measurable change was seen in the presence of 3 mM Ca^{2+}. This suggests the presence of at least one Ca^{2+}-masked soluble lipid binding site in the Gla domain of bovine factor X_a but no Ca^{2+}-dependent site. This site was not specific for PS, because C6PC also bound to the Gla domain in the absence of Ca^{2+} (data not shown).

Ca^{2+} bound to the EGF_N domain of factor X_a and induced a large decrease in the ellipticity ratio (81%) but no change in the α-helical content (Table II). This is not surprising, because the solution structure of bovine factor X_a EGF_N is reported to consist almost entirely of anti-parallel β-sheets and turns (39) and Ca^{2+} binding to Gla-EGF_N seems not to alter its fold (19). This is another example of how the $\Theta_{222}/\Theta_{208}$ ratio reflects more than the α-helical content of a protein, and, in this case, must reflect Ca^{2+}-induced structural rearrangements that alter the electronic symmetry of EGF_N. By contrast to Ca^{2+}, C6PS had no effect on the EGF_N spectrum (data not shown)

TABLE III
Stoichiometry determination for soluble C6PS binding to various fragments of human and bovine factor X_a in the presence and absence of 3 mM Ca^{2+}

Species	Stoichiometry	C6PS concentration used
		μM
3 mM Ca^{2+}		
Human X_a	1.75 ± 0.03	400
Human $GDFX_a$	1.96 ± 0.09	600
Bovine Gla-EGF_{NC}	0.97 ± 0.07	400
Bovine Gla	NC[a]	400
No Ca^{2+}		
Human X_a	0.93 ± 0.07	400
Human $GDFX_a$	NC[a]	600
Bovine Gla-EGF_{NC}	1.76 ± 0.05	800
Bovine Gla	0.96 ± 0.12	400

[a] No change in lipid concentration detected between two chambers, *i.e.* no binding detected.

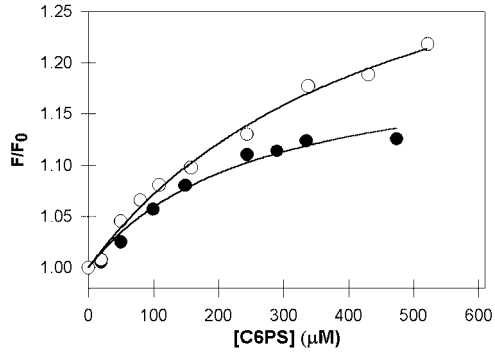

FIG. 5. **Response of Gla-EGF_{NC} intrinsic fluorescence to titration by soluble C6PS.** 100 nM bovine Gla-EGF_{NC} was titrated with soluble C6PS in a buffer containing 50 mM Tris, 150 mM NaCl at pH 7.4 in the presence of 3 mM Ca^{2+} (*closed circles*) and in the absence of Ca^{2+} (*open circles*). Fluorescence intensities of Gla-EGF_{NC} were measured following an equilibrium period of 4 min after each addition of C6PS. The *curves* passing through the data were obtained by fitting the data to a single binding site model (see "Methods"), yielding dissociation constants for C6PS binding to Gla-EGF_{NC} in the presence and in the absence of Ca^{2+} of 203 and 470 μM, respectively.

either in the presence or in the absence of Ca^{2+} (Table II). The Gla-EGF_N domain pair also bound to Ca^{2+} and induced a 140% increase in ellipticity ratio (Fig. 4*E*). In terms of secondary structure, this translated into a large increase in $\Theta_{222}/\Theta_{208}$ and a nearly insignificant decrease in α-helical content (Tables I and II). It is known from NMR studies that Gla-EGF_N undergoes a significant structural reorganization in which the EGF and Gla domains fold onto each other upon binding Ca^{2+} (19). C6PS induced a structural change in Gla-EGF_N in the absence of Ca^{2+} ($\Theta_{222}/\Theta_{208}$ increased by 333% and helicity increased by 2.3%; Fig. 4*E* and Table II), but no C6PS-dependent change was detected in the presence of 3 mM Ca^{2+}. The change in $\Theta_{222}/\Theta_{208}$ seen in the absence of Ca^{2+} was much greater than seen for the Gla domain (Table II). Because EGF_N showed no change in response to C6PS, this implies that C6PS binding to Gla-EGF_N in the absence of Ca^{2+}, like the binding of Ca^{2+} in the absence of C6PS (19), involves linkage between the Gla and EGF_N domains.

Unlike Gla-EGF_N, Gla-EGF_{NC} interacted with soluble C6PS in the presence of Ca^{2+} ($\Theta_{222}/\Theta_{208}$ increased by a barely perceptible 10% while helicity also increased by only 1.1%) as well as in its absence ($\Theta_{222}/\Theta_{208}$ and helicity increased by 121 and 2.8%, respectively).

Stoichiometry of C6PS Binding to Factor X_a and Its Fragments—To test and extend our CD observations, C6PS binding to bovine and human factor X_a and their fragments was also monitored by equilibrium dialysis, a direct binding measurement. Because of the large quantities of protein needed for these measurements, it was not possible to obtain complete binding isotherms by this method. However, using dissociation constants estimated from our CD data, it was possible to estimate binding stoichiometries (see Equation 1 under "Methods"). The measured stoichiometries of C6PS binding to various fragments in the presence and in the absence of 3 mM Ca^{2+} are shown in Table III. Human factor X_a binds two molecules of C6PS in the presence and one in the absence of 3 mM Ca^{2+}, respectively, just like bovine factor X_a.[2] Human Gla domainless factor X_a ($GDFX_a$) also bound two molecules of C6PS in the presence of Ca^{2+} but did not bind to C6PS in the absence of Ca^{2+}. The bovine Gla domain bound one molecule of C6PS in the absence of Ca^{2+} and did not bind C6PS in the presence of 3 mM Ca^{2+}, consistent with the lack of any change in $\Theta_{222}/\Theta_{208}$ under these conditions (Fig. 4*D*). When the Gla domain was linked to the EGF_{NC} domain, it bound two molecules of C6PS in the absence and one molecule of C6PS in the presence of 3 mM Ca^{2+}. Stoichiometry measurements were thus all consistent with the results of our CD experiments. Together, these results provide a clear and self-consistent picture of the distribution of C6PS binding sites on factor X_a (Fig. 1).

Fluorescence of Gla-EGF_{NC} Titrated with C6PS—Because the C6PS-induced change in secondary structure in the Gla-EGF_{NC} domain triplet was so small (Fig. 4*F*), we tested further for a C6PS-induced conformational change by titrating the intrinsic fluorescence of Gla-EGF_{NC} with soluble C6PS in the absence (*open circles*) and presence (*closed circles*) of 3 mM Ca^{2+}, with the results shown in Fig. 5. The curves passing through the data were obtained by fitting the data to the single binding site model (see "Methods"). The apparent stoichiometric binding constants for C6PS binding to Gla-EGF_{NC} in the presence and absence of Ca^{2+} were 203 ± 63 and 470 ± 74 μM, respectively. These binding constant are comparable to those obtained by CD measurements (Table II). We conclude that Ca^{2+}-dependent binding of C6PS produced conformational changes in the Gla-EGF_{NC} domain triplet.

Fluorescence of DEGR-E_2FX_a Titrated with C6PS—Although CD data suggest that a Ca^{2+}-requiring site might be located in the E_2FX_a fragment, we could not confirm this by direct stoichiometry measurement due to a lack of sufficient quantities of this expressed protein. To confirm the Ca^{2+}-requiring binding site in to the E_2FX_a fragment, we labeled E_2FX_a with DEGR-CK and monitored the change of fluorescence intensity of DEGR-E_2FX_a as a function of C6PS. The binding analysis was performed with two preparations of DEGR-E_2FX_a, and the results are presented in Fig. 6, with the results from the two preparations distinguished by *closed circles* and *closed squares*. The results clearly show a saturable drop in DEGR- E_2FX_a fluorescence in the presence of Na^+ and Ca^{2+}, although no change was detected when either Ca^{2+} (*open triangles*) or Na^+ (*open circles*) were missing. This requirement for Na^{2+} and Ca^{2+} for C6PS binding to E_2FX_a raises the possibility that the site in the E_2FX_a fragment might be the amine binding site that is also reported to require Ca^{2+} and Na^+ (40). A global fit of a single-site binding model to the two data sets obtained in the presence of both Na^{2+} and Ca^{2+} is shown by the solid hyperbolic curve.

Effect of Soluble C6PS on the Amidolytic Activities of Expressed Human GDFXa and Its Mutant Y99T—To better establish the identity of the C6PS site located in the E_2FX_a fragment, we monitored hydrolysis of SpPCa by $GDFX_a$ and its mutant Y99T as a function of soluble C6PS, in buffer lacking Ca^{2+}. Monnaie *et al.* (40) showed that an amine binding site

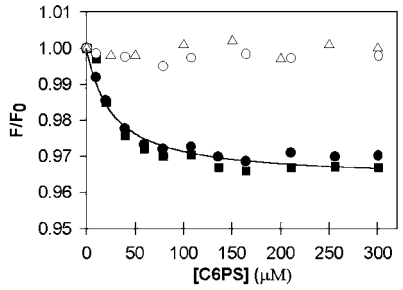

FIG. 6. **Response of DEGR-E_2FX_a fluorescence to titration by soluble C6PS.** 100 nM human DEGR-E_2FX_a was titrated with soluble C6PS in buffers: 50 mM Tris, 3 mM $CaCl_2$, and 150 mM NaCl (*closed circles* and *closed squares* representing two independent preparations of DEGR-E_2FX_a); 50 mM Tris, 3 mM $CaCl_2$ (*open circles*); and 50 mM Tris, 150 mM NaCl (*open triangles*) at pH 7.4. Fluorescence intensities were measured 4 min after each addition of C6PS. A global fit of a single-site binding model to the two data sets obtained in the presence of both Na^{2+} and Ca^{2+} is shown by the *solid hyperbolic curve* and yielded a dissociation constant of 27 ± 5 μM.

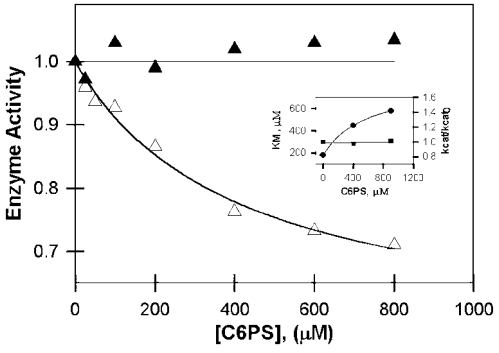

FIG. 7. **The effect of soluble C6PS on the amidolytic activities of expressed human GDFX_a and its mutant Y99T.** The initial rates of SpPCa amidolysis by GDFX_a (*closed triangles*) and Y99T (*open triangles*) in the absence of Ca^{2+} are plotted as a function of C6PS concentrations. Rates were measured at 37 °C in a buffer containing 50 mM Tris, 175 mM NaCl, 0.6% PEG, at pH 7.6. The *hyperbolic line* passing through the Y99T data was obtained by fitting the data to the single-binding-site model, which yielded a dissociation constant of 410 ± 88 μM. The initial rates of Y99T amidolysis were determined at 0, 400, and 900 μM C6PS concentrations and at 50, 100, 200, 400, and 600 μM substrate concentrations. From these data, we determined the k_{cat} and K_M values for SpPCa amidolysis by Y99T at these three lipid concentrations. The variation of k_{cat}/k_{cat0} (*circles*) and K_M (*squares*) with the C6PS concentration is shown in the *inset*.

exists in the catalytic domain and shares at least some residues with the substrate binding site. Like binding of C6PS, this site was both Ca^{2+}- and Na^+-dependent. The variation of amidolytic activities as a function of C6PS concentrations is shown in Fig. 7. As expected, because no C6PS binding site was detected in GDFXa in the absence of Ca^{2+}, soluble C6PS did not have any effect on the rate of hydrolysis of SpPCa by GDFX_a (*closed triangles*). However, the rate of hydrolysis of SpPCa by the Y99T GDFX_a mutant decreased with the addition of C6PS, and the binding curve (*open triangles*) was fitted to a single-binding-site model with an apparent stoichiometric dissociation constant of 410 μM. It appears that the Ca^{2+}-requiring C6PS binding site in GDFX_a becomes independent of Ca^{2+} as a result of the Y99T mutation. This result clearly proves that residue Tyr-99, which is known to be part of a reported amine binding site and the substrate binding site (40), plays a role in C6PS binding to the Ca^{2+}-requiring site located in the E_2FX_a fragment. The question still remains: Are the C6PS site and the substrate binding site are one and the same? To answer this question, we monitored the effect of C6PS on the k_{cat} and K_M for SpPCa hydrolysis by Y99T GDFX_a in the absence of Ca^{2+}. As shown in the *inset* in Fig. 7, k_{cat} remained constant with C6PS concentration but K_M increased in a hyperbolic fashion with an increase in lipid concentration. This means that C6PS competes with substrate for the substrate binding site, just as tertiary amines have been shown to do (40). We conclude that the Ca^{2+}-requiring C6PS binding site shares some ligand-recognition residues with the substrate binding site. We report elsewhere that the Ca^{2+}-requiring site minimally recognizes glycerolphosphorylserine and does not bind phosphatidylcholine.[3] Because the amine binding site recognizes choline (40), it is unlikely that the C6PS site and the amine site are identical, but they likely share some ligand recognition regions with each other and with the substrate binding site.

DISCUSSION

We have shown previously (1) that soluble C6PS enhanced factor X_a's proteolytic activity by about 60- to 70-fold. The purpose of this work was to locate the C6PS effector sites to one or more domains of factor X_a. Our results have located three sites on this serine protease but suggest that only one is involved in functional regulation. These results support a reasonable hypothesis for how one molecule of regulatory C6PS and two molecules of non-regulatory C6PS are bound to factor X_a. This hypothesis is summarized in Fig. 1. The arguments in favor of this hypothesis are summarized below.

One Ca^{2+}-masked Phospholipid Site Is Located in the Gla Domain—As expected (42), the secondary structure of the Gla domain was sensitive to the presence of 3 mM Ca^{2+} (compare *open* and *closed circles* of Fig. 4ID at 0 mM C6PS) with the change elicited by Ca^{2+} being a 43% increase in $\Theta_{222}/\Theta_{208}$ and a 1.8% increase in α-helical content. However, the C6PS site in the Gla domain was masked by Ca^{2+}, because no structural response was seen (Fig. 4*D*). This is surprising, because binding of Gla-containing proteins to PS-containing membranes has long been seen as mediated by a Ca^{2+}-induced conformational change of the Gla domain (43–46). It may be that binding of Gla-containing proteins to a PS-containing membrane involves adsorption of the Ca^{2+}-conformation of the Gla domain to a membrane surface (31, 47–48) rather than recognition of individual PS molecules by specific binding sites. By contrast, the C6PS-induced conformational change that we see in the absence of Ca^{2+} does involve a single C6PS molecule (Table III). Because neither human (1) nor bovine factor X_a[2] respond functionally to C6PS in the absence of Ca^{2+}, it is unlikely that this Ca^{2+}-masked site could by itself be a regulatory site.

Two C6PS Sites Exist in the Factor X_a Fragment that Lacks the Gla Domain (GDFX_a)—Our stoichiometry measurements showed that GDFX_a binds two molecules of C6PS in the presence of 3 mM Ca^{2+} (Table III). Both of these sites are Ca^{2+}-dependent, because there was no detectable change in $\Theta_{222}/\Theta_{208}$ (Fig. 4*B*, *open circles*), and the stoichiometry was nearly zero (Table III) in the absence of Ca^{2+}, meaning binding of C6PS in the absence of Ca^{2+} is at best quite weak.

The EGF and Gla Domains Are Structurally Linked by C6PS Binding—The EGF_N domain alone did not respond structurally to C6PS, in either the presence or absence of Ca^{2+} (Table II). In the absence of Ca^{2+}, however, when linked covalently to the Gla domain, the EGF_N domain either experienced a large conformational change ($\Delta\Theta_{222}/\Theta_{208}$ = 333%) or modified in a major way the response of the Gla domain ($\Delta\Theta_{222}/\Theta_{208}$ = 97%) to C6PS. Based on a comparison of the structural changes for Gla and Gla-EGF_N and on the low helical content of these two domains in homologous factor IX_a (8), it would appear most likely that the response being monitored in Gla-EGF_N is not

[3] M. Banerjee, D. C. Drummond, A. Srivastava, D. Daleke, and B. R. Lentz, submitted for publication.

that of the Gla domain and is not a change in α-helix content, but is a change in the EGF_N module that requires conformational linkage to the Gla domain. Like Gla, Gla-EGF_N did not bind C6PS in the presence of Ca^{2+}, so the Gla-EGF_N site seen in the absence of Ca^{2+} must involve the Ca^{2+}-masked site in the Gla domain. Ca^{2+}-mediated conformational linkage between the Gla and EGF_N domains of factor X_a is well established (14, 19), and our results imply that this linkage involves a C6PS binding site as well.

Unlike the Gla-EGF_N fragment, the Gla-EGF_{NC} fragment experienced a structural change induced by C6PS both in the presence and absence of Ca^{2+}, although the changes seen in the presence of Ca^{2+} were qualitatively different from those seen in its absence (Figs. 4*F* and 5). Stoichiometry measurements showed that Gla-EGF_{NC} binds one C6PS molecule in the presence of Ca^{2+} and two in the absence of Ca^{2+} (Table III). Based on these observations, Gla-EGF_{NC} seems to have two types of C6PS sites. One is the Ca^{2+}-masked site in the Gla domain, and one is a site that does not require Ca^{2+} to recognize C6PS but that binds C6PS much more tightly in the presence of Ca^{2+} than in its absence (Table II and Fig. 5). The Ca^{2+}-dependent site requires linkage of all three N-terminal modules (Gla, EGF_N, and EGF_C) for a full response. Ca^{2+} is known to link the EGF_N and Gla domains (14, 19), and Ca^{2+} masks the C6PS site in the Gla domain. For these reasons, we suggest that Ca^{2+} links the C6PS sites in the Gla-EGF_N and EGF_{NC} domains to create one site having higher affinity for C6PS than either of the individual sites. If so, we expect that the sandwich formed by the Ca^{2+}-linked Gla and EGF_N domains (19) will form an important element of this binding site.

A Ca^{2+}-requiring Site in the EGF_C-catalytic Domain Is Probably Part of the Substrate Recognition Site—Direct measurement of stoichiometry by equilibrium dialysis measurements showed two C6PS binding sites in $GDFX_a$ in the presence of Ca^{2+} and none in the absence of Ca^{2+} (Table III). We know that one of these Ca^{2+}-dependent sites must be in the EGF_{NC} pair. A Ca^{2+}-requiring site is in the E_2FX_a fragment (Figs. 4*C* and 6). Our experiment with the Y99T mutant of $GDFX_a$ showed that C6PS binding to the Ca^{2+}-requiring site in the E_2FX_a fragment competes with binding of substrate (*inset* to Fig. 7). In addition, C6PS binding to $GDFX_a$ was altered by the Y99T mutation and Y99 is known to be part of the substrate recognition site (40). From these observations, we conclude that the Ca^{2+}-requiring C6PS site in E_2FX_a at least overlaps the substrate recognition site. This is consistent with the fact that substrate recognition is also linked to Na^+ and Ca^{2+} binding (35, 36). Because this site is located roughly 60 Å from the membrane surface (37), it is unlikely to be involved in regulating activity *in vivo*.

The Functional Response to C6PS Seems to Require Minimally the EGF_{NC} Pair and the Catalytic Domain—It is known that the proteolytic activity of factor X_a is enhanced roughly 60- to 70-fold by binding of C6PS (1). The change in amidolytic activity of the $GDFX_a$ fragment upon titration with C6PS clearly followed a single-site-binding model (Fig. 2), suggesting either that only one site regulates activity or that the two sites are equivalent in their abilities to modulate activity. This fragment consists of a pair of EGF-like domains and a catalytic domain. Our data show that one C6PS site is located at or near the substrate recognition site (Fig. 7) and that one site is most likely in the EGF_{NC} pair (Fig. 1 and Tables I–III). It appears for three reasons that regulation of activity by C6PS requires the site in the EGF_{NC} pair. First, the substantial amidolytic activity toward S-2765 of the E_2FX_a fragment did not respond to C6PS (Fig. 2), although E_2FX_a did undergo a C6PS-induced conformational change that required Ca^{2+} (Fig. 6). Second, the K_d for the Ca^{2+}-dependent structural response of bovine Gla-EGF_{NC} to C6PS (155 μM, Table II) was similar to that for the activity response of bovine factor X_a (167 μM).[2] Finally, the site in the EGF_{NC} pair can be occupied in the presence or absence of Ca^{2+} (see Figs. 4*F* and 5 and Table II), but with very different K_d values and structural responses under these two circumstances (Table II). In the absence of Ca^{2+}, the response to C6PS seems to depend only on the linkage of Gla to EGF_N, while in the presence of Ca^{2+}, the complete EGF_{NC} pair is needed. Because factor X_a is active only in the presence of Ca^{2+}, we conclude that the site that regulates activity requires both the EGF domains. The fact that the response of $GDFX_a$ activity to C6PS was only about a tenth that of whole factor X_a implies that the regulatory site is in the EGF_{NC} domain but that linkage to the Gla domain is essential for optimal changes in the catalytic domain's active site.

Bovine and Human Factor X_a Have Analogous C6PS Binding Sites—Based on our results, we have noted that the bovine and human forms of factor X_a show different structural responses to C6PS despite having very similar secondary structures in solution. If their responses to C6PS are different, it could also be that the location of C6PS binding sites might be different and our use of data from both bovine N-terminal fragments (Gla, Gla-EGF_N, and Gla-EGF_{NC}) and human C-terminal biosynthetic fragments from cDNA constructs (X_a, $GDFX_a$, E_2FX_a) would be flawed. Based on the analysis provided below that is based on careful inspection of the diagram in Fig. 1 summarizing all our observations, we argue that this is not the case.

Data obtained with the *human X fragments* clearly show that a single Ca^{2+}-requiring C6PS site exists in E_2FX_a. The existence of this site in the catalytic domain was confirmed by our titration of DEGR-E_2FX_a fluorescence in the absence of Na^+ and by titration of the activity of the Y99 mutant of $GDFX_a$ in the absence of Ca^{2+}. Titrations of the amidolytic activity of these biosynthetic human factor X_a fragments show that another site exists in the EGF_{NC} pair and this site regulates factor X_a activity. This second site was either absent or too weak to be detected in the absence of Ca^{2+}. Because a single C6PS bound to whole factor X_a and none bound to $GDFX_a$ in the absence of Ca^{2+}, there must be a Ca^{2+}-masked C6PS binding site in the Gla domain. The very different responses of whole factor X_a and $GDFX_a$ in the presence of Ca^{2+} (Fig. 2) to C6PS shows that linkage of the Gla and EGF_{NC} modules is needed for a full functional response.

If we consider the experiments done with *N-terminal fragments of bovine factor X_a*, we see clearly that a Ca^{2+}-masked C6PS site exists in the Gla domain. We see as well that a single Ca^{2+}-dependent (but not requiring) site exists in Gla-EGF_{NC}. This site requires the linkage of the Gla, EGF_N, and EGF_C modules. Because two C6PS bind to whole bovine factor X_a in the presence of Ca^{2+}, there must be a second site in the catalytic domain.

We argue from this analysis that data obtained with bovine and human fragments lead independently to nearly the same conclusions. This means both that the bovine and human proteins interact similarly with C6PS (as expected for such highly homologous proteins) and that the two sets of data with proteins from different species support and confirm each other.

REFERENCES

1. Koppaka, V., Wang, J., Banerjee, M., and Lentz, B. R. (1996) *Biochemistry* **35,** 7482–7491
2. Sandberg, H., Bode, A. P., Dombrose, F. A., Hoechli, M., and Lentz, B. R. (1985) *Thromb. Res.* **39,** 63–79
3. Sims, P. J., Faioni, E. M., Wiedmer, T., and Shattil, S. J. (1988) *J. Biol. Chem.* **263,** 18205–18212
4. Stenflo, J. (1991) *Blood* **78,** 1637–1651
5. Padmanabhan, K., Padmanabhan, K. P., Tulinsky, A., Park, C. H., Bode, W., Huber, R., Blankenship, D. T., Cardin, A. D., and Kisiel, W. (1993) *J. Mol. Biol.* **232,** 947–966

6. Brandstetter, H., Kuhne, A., Bode, W., Huber, R., von der Saal, W., Wirthensohn, K., and Engh, R. A. (1996) *J. Biol. Chem.* **271,** 29988–29992
7. Kamata, K., Kawamoto, H., Honma, T., Iwama, T., and Kim, S. H. (1998) *Proc. Natl. Acad. Sci. U. S. A.* **95,** 6630–6635
8. Brandstetter, H., Bauer, M., Huber, R., Lollar, P., and Bode, W. (1995) *Proc. Natl. Acad. Sci. U. S. A.* **92,** 9796–9800
9. Sabharwal, A. K., Padmanabhan, K., Tulinsky, A., Mathur, A., Gorka, J., and Bajaj, S. P. (1997) *J. Biol. Chem.* **272,** 22037–22045
10. Jesty, J., and Nemerson, Y. (1976) *Methods Enzymol.* **45,** 95–107
11. Fujimura, H., Kambayash, J., Monden, M., Kato, H., and Miyata, T. (1995) *Thromb. Haemost.* **74,** 1381–1382
12. Handford, P. A., Mayhew, M., Baron, M., Winship, P. R., Campbell, I. D., and Brownlee, G. G. (1991) *Nature* **351,** 164–167
13. Henriksen, R. A., and Jackson, C. M. (1975) *Arch. Biochem. Biophys.* **170,** 149–159
14. Persson, E., Selander, M., Linse, S., Drakenberg, T., Ohlin, A. K., and Stenflo, J. (1989) *J. Biol. Chem.* **264,** 16897–16904
15. Rezaie, A. R., and Esmon, C. T. (1994) *J. Biol. Chem.* **269,** 21495–21499
16. Rezaie, A. R., Neuenschwander, P. F., Morrissey, J. H., and Esmon, C. T. (1993) *J. Biol. Chem.* **268,** 8176–8180
17. Persson, E., Hogg, P. J., and Stenflo, J. (1993) *J. Biol. Chem.* **268,** 22531–22539
18. Valcarce, C., Holmgren, A., and Stenflo, J. (1994) *J. Biol. Chem.* **269,** 26011–26016
19. Sunnerhagen, M., Olah, G. A., Stenflo, J., Forsen, S., Drakenberg, T., and Trewhella, J. (1996) *Biochemistry* **35,** 11547–11559
20. Mann, K. G. (1976) *Methods Enzymol.* **45,** 123–156
21. Tendian, S. W., and Lentz, B. R. (1990) *Biochemistry* **29,** 6720–6729
22. Dahlback, B., and Stenflo, J. (1980) *Eur. J. Biochem.* **104,** 549–557
23. Nossel, H. (1964) *Thromb. Diath. Haemorrh.* **12,** 505–518
24. Jameson, G. W., Roberts, D. V., Adams, R. W., Kyle, W. S., and Elmore, D. T. (1973) *Biochem. J.* **131,** 107–117
25. Persson, E., Valcarce, C., and Stenflo, J. (1991) *J. Biol. Chem.* **266,** 2453–2458
26. Valcarce, C., Persson, E., Astermark, J., Ohlin, A. K., and Stenflo, J. (1993) *Methods Enzymol.* **222,** 416–435
27. Morita, T., and Jackson, C. M. (1986) *J. Biol. Chem.* **261,** 4015–4023
28. Vindigni, A., Winfield, M., Ayala, Y. M., and Di Cera, E. (2000) *Protein Sci.* **9,** 619–622
29. Rezaie, A. R. (1996) *J. Biol. Chem.* **271,** 23807–23814
30. Guinto, E. R., Vindigni, A., Ayala, Y. M., Dang, Q. D., and Di Cera, E. (1995) *Proc. Natl. Acad. Sci. U. S. A.* **92,** 11185–11189
31. Ellison, E. H., and Castellino, F. J. (1997) *Biophys. J.* **72,** 2605–2615
32. Greenfield, N. J. (1996) *Anal. Biochem.* **235,** 1–10
33. Sreerama, N., and Woody, R. W. (2000) *Anal. Biochem.* **287,** 252–260
34. Johnson, W. C., Jr. (1990) *Proteins* **7,** 205–214
35. Underwood, M. C., Zhong, D., Mathur, A., Heyduk, T., and Bajaj, S. P. (2000) *J. Biol. Chem.* **275,** 36876–36884
36. Rezaie, A. R., and He, X. (2000) *Biochemistry* **39,** 1817–1825
37. Husten, E. J., Esmon, C. T., and Johnson, A. E. (1987) *J. Biol. Chem.* **262,** 12953–12961
38. Chen, P. S., Jr., Toribara, T. Y., and Warner, H. (1956) *Analyt. Chem.* **28,** 1756–1758
39. Ullner, M., Selander, M., Persson, E., Stenflo, J., Drakenberg, T., and Teleman, O. (1992) *Biochemistry* **31,** 5974–5983
40. Monnaie, D., Arosio, D., Griffon, N., Rose, T., Rezaie, A. R., and Di Cera, E. (2000) *Biochemistry* **39,** 5349–5354
41. Deleted in proof
42. Sunnerhagen, M., Forsen, S., Hoffren, A. M., Drakenberg, T., Teleman, O., and Stenflo, J. (1995) *Nat. Struct. Biol.* **2,** 504–509
43. Nelsestuen, G. L., Broderius, M., and Martin, G. (1976) *J. Biol. Chem.* **251,** 6886–6893
44. Lim, T. K., Bloomfield, V. A., and Nelsestuen, G. L. (1977) *Biochemistry* **16,** 4177–4181
45. Schwalbe, R. A., Ryan, J., Stern, D. M., Kisiel, W., Dahlback, B., and Nelsestuen, G. L. (1989) *J. Biol. Chem.* **264,** 20288–20296
46. Pearce, K. H., Hof, M., Lentz, B. R., and Thompson, N. L. (1993) *J. Biol. Chem.* **268,** 22984–22991
47. Lecompte, M. F., and Miller, I. R. (1980) *Biochemistry* **19,** 3439–3446
48. McDonald, J. F., Shah, A. M., Schwalbe, R. A., Kisiel, W., Dahlback, B., and Nelsestuen, G. L. (1997) *Biochemistry* **36,** 5120–5127